Journal of Alloys and Compounds 520 (2012) 250–254

Contents lists available at SciVerse ScienceDirect

Journal of Alloys and Compounds

journal homepage: www.elsevier.com/locate/jallcom

# Effect of incorporating copper on resistive switching properties of ZnO films

C.H. Jia, Q.C. Dong, W.F. Zhang *

*Key Laboratory of Photovoltaic Materials of Henan Province and School of Physics Electronics, Henan University, Kaifeng 475004, PR China*

ARTICLE INFO

*Article history:*
Received 10 October 2011
Received in revised form 5 January 2012
Accepted 5 January 2012
Available online 13 January 2012

*Keywords:*
ZnO:Cu
Resistive switching

ABSTRACT

Undoped and copper-doped ZnO (ZnO:Cu) thin films of wurtzite structure with *c*-axis orientation were grown on F-doped $SnO_2$ (FTO) substrates by pulsed laser deposition. Typical bipolar and reversible resistance switching effects were observed in these films, and the ratio of high and low resistance state (ON/OFF ratio) increases abruptly by introducing Cu. Based on the impedance spectra of ZnO and ZnO:Cu films, the change of resistance at high and low resistance states is found to be accompanied with the variance of depletion width. Furthermore, the depletion width of ZnO films changes little, while that of ZnO:Cu films varies greatly under different resistance states, which is consistent with the result of that ZnO:Cu films show a much larger ON/OFF ratio than ZnO films. Therefore, the resistance switchings are supposed to be due to the change of depletion width of Schottky barrier.

© 2012 Elsevier B.V. All rights reserved.

## 1. Introduction

Electric field induced resistive switching (RS) has attracted lots of interest because of its potential applications in the resistive random access memory (ReRAM) devices [1,2]. In the operation of ReRAM devices, an external electric field switches the resistance reversibly between a high resistance state (HRS) and a low resistance state (LRS) to realize the data storage. Resistive switching effects have been found in various materials, including solid electrolytes, perovskites, binary transition metal oxides (TMO), amorphous silicon, and even organics [3]. Among them, binary TMO have many advantages, such as simple composition, low deposition temperature and compatible with complementary metal oxide semiconductor processes, making them promising candidates for practical applications of ReRAM. As one of the most important binary TMO at present, ZnO has wide applications in electronics, optics, optoelectronics, spintronics and energy generators, which can be achieved through band gap engineering, dopant incorporation, defect engineering, or heterostructure engineering [4,5]. For the doped ZnO compounds, copper-doped ZnO (ZnO:Cu) has captured considerable attention in magnetic semiconductors [6], light emitting diodes [7], surface acoustic wave [8], and optical switching [9,10] applications. Cu ions are well known as electron traps in ZnO films and they can increase the resistivity of ZnO from semiconducting to insulating-like properties [10–12]. More importantly, the Cu dopants was found to be efficient for realizing stable p-type ZnO films [13]. These notable characteristics of ZnO:Cu have attracted our interest to explore its potential use in ReRAM. However, up to our knowledge, there is little report on the resistive switching properties of ZnO:Cu films.

In this paper, we report that ZnO:Cu thin films grown on fluorine doped tin oxide (FTO) coated glass substrates by pulsed laser deposition (PLD) show bipolar RS behavior. By fitting the current–voltage curves and impedance spectra, the resistance switching in both ZnO and ZnO:Cu films are supposed to be due to the change in depletion width of Schottky barrier.

## 2. Experiments

Commercial glass coated by about 150 nm thick FTO layer was used as substrate and bottom electrode simultaneously, which is promising for transparent nonvolatile memory devices. Before loading into the deposition chamber, the FTO substrates were cleaned using acetone, alcohol, and then washed in deionized water. A pulsed KrF excimer laser (COMPexPro201, Coherent) with a wavelength of 248 nm, pulse duration of 25 ns, frequency of 5 Hz, and a lens of focal length of 300 mm was focused on the sintered ZnO and ZnO:Cu (doped with 9% of Cu) ceramic targets with a purity of 99.99%. ZnO and ZnO:Cu films were deposited at a substrate temperature of 500 °C, while the vacuum maintained at $5 \times 10^{-4}$ Pa without introducing oxygen and/or nitrogen. The nominal thickness is about 100 nm for ZnO and ZnO:Cu films. The crystal structures of ZnO and ZnO:Cu films are characterized by X-ray diffraction (XRD, DX2500). The Cu element was verified to be present in ZnO:Cu thin film by X-ray photoelectron spectroscopy (XPS, KRATOS, AXIS ULTRA). The surface images of ZnO and ZnO:Cu films are performed by atomic force microscope (AFM, NT-MDT, Solver pro p47 h). The Hall effect was measured by van der Pauw method (Ecopia, HMS-3000). The resistivity, Hall mobility and carrier concentration are $1.84 \times 10^{-2}$ and $2.18 \times 10^{-1}$ Ω cm, 12.8 and

* Corresponding author. Tel.: +86 378 3881940; fax: +86 378 3880659.
*E-mail address:* wfzhang@henu.edu.cn (W.F. Zhang).

0925-8388/$ – see front matter © 2012 Elsevier B.V. All rights reserved.
doi:10.1016/j.jallcom.2012.01.035

$3.8\,cm^2/V{\cdot}s$, $2.6 \times 10^{19}$ and $7.6 \times 10^{18}\,cm^{-3}$ for ZnO and ZnO:Cu films, respectively. For electrical measurements, Au top electrodes with 0.2 mm in diameter were sputtered on the thin films through a shadow mask. Keithley 2400 sourcemeter was used to conduct the transport measurements. Agilent 4294A was used to measure the complex impedance spectroscopy in a frequency range from 40 Hz to 10 MHz with a fixed oscillating voltage of 500 mV at HRS and LRS, respectively. A forward (positive) bias applied to the device is defined as the current flowing from the top Au electrode into the film. All the characterizations and measurements were performed at room temperature.

## 3. Results and discussion

Fig. 1(a) shows the XRD patterns of ZnO and ZnO:Cu films on FTO substrates. The samples exhibit a pure wurtzite structure of *c*-axis orientation without detectable secondary phase. From the XPS spectra of ZnO and ZnO:Cu films on Si substrates, as shown in Fig. 1(b), it can be seen that the copper element is present in ZnO:Cu films but not in ZnO, just as expected. The peaks at 932.44 and 951.43 eV is corresponding to Cu $2p_{3/2}$ and Cu $2p_{1/2}$, while the energy separation of 19 eV is the typical character of spin–orbit interaction [14]. From the AFM images of ZnO and ZnO:Cu films, as shown in Fig. 1(c and d), it is clear that ZnO grains have a strong tendency to agglomerate, but not in ZnO:Cu films. This phenomenon has also been found in indium doped $Bi_4Ti_3O_{12}$ films [15]. Obviously, the introduction of copper element is efficient to improve the surface smoothness.

In the Au/ZnO/FTO and Au/ZnO:Cu/FTO configurations shown in Fig. 2(a), resistance switching (RS) was observed without a forming process, as shown in Fig. 2(b and c). The sweeping direction of voltage is $0\,V \to 7\,V \to 0\,V \to -7\,V \to 0\,V$, named as '1′–'4′ section, and the sweep speed is 0.3 V/s. Such a reverse bias modulation is a typical character of bipolar RS, since a reverse bias sweeping is needed to drive the device to HRS, while another forward voltage sweeping switches it back to LRS [16]. Furthermore, it is clear that the ratio of HRS and LRS, that is the ON/OFF ratio, increases greatly with introducing copper element in ZnO films. This phenomenon has also been found in Mn doped ZnO films [17]. It was proposed that the transition metal doping can reduce the intrinsic carrier density due to the trapping of the free electrons by the Cu-related defect states [9,10], which is consistent with the Hall effect in the present work, and compensate the intrinsic donors of oxygen vacancy and zinc interstitial, which helps to increase the ON/OFF ratio.

For both ZnO and ZnO:Cu films, the LRS follows the Ohmic behavior, while the HRS shows a nonlinear curve. To investigate the origin of the switching behaviors, we carried out nonlinear fittings to the transport characteristics. For nonlinear current–volatge curves, we have considered three meachanisms as follows: space-charge-limited (SCL) conduction, Poole–Frenkel (P–F) emission, and Schottky emission. The validity of the fittings is usually determined by the derived refractive index [17–19]. For SCL conduction, the *I*–*V* curve first follows the Ohmic's law and then the Child's law as follow: $I \propto (9/8)\varepsilon_r\varepsilon_0\mu S(V^2/d^3)$, where $I$ is the current, $\varepsilon_r$ is the relative dielectric constant, $\varepsilon_0$ is the permittivity of free space, $\mu$ is the mobility of charge carriers, $S$ is the area of electrode, $V$ is the voltage, and $d$ is the film thickness. From the SCL emission fittings shown in Fig. 2(d and e), the relative dielectric constants for ZnO and ZnO:Cu films are derived to be $6.0 \times 10^{-3}$ and $2.4 \times 10^{-2}$, respectively. Thus the refractive indexes for ZnO and ZnO:Cu films are 0.077 and 0.15, respectively, which are much smaller than

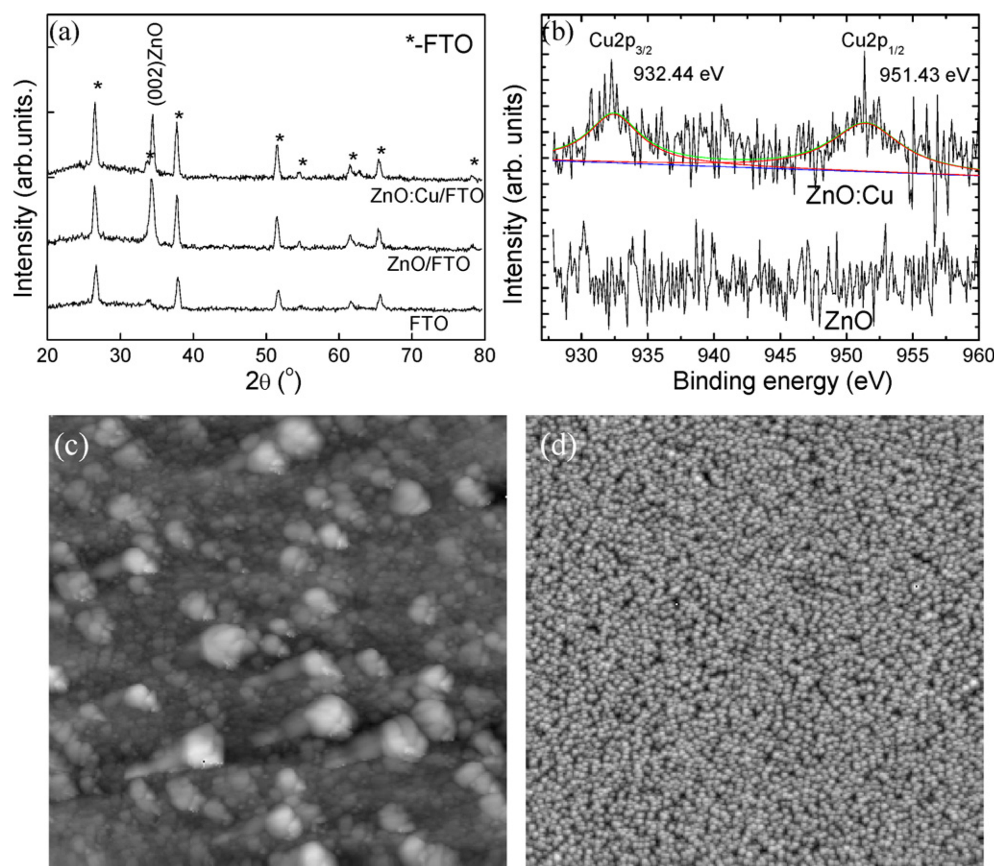


**Fig. 1.** XRD patterns of ZnO and ZnO:Cu thin films deposited on FTO substrates (a); Cu 2p ore level spetra of ZnO and ZnO:Cu thin films deposited on Si (b); AFM images ($5 \times 5\,\mu m^2$) of ZnO (c) and ZnO:Cu (d) thin films deposited on FTO substrates.

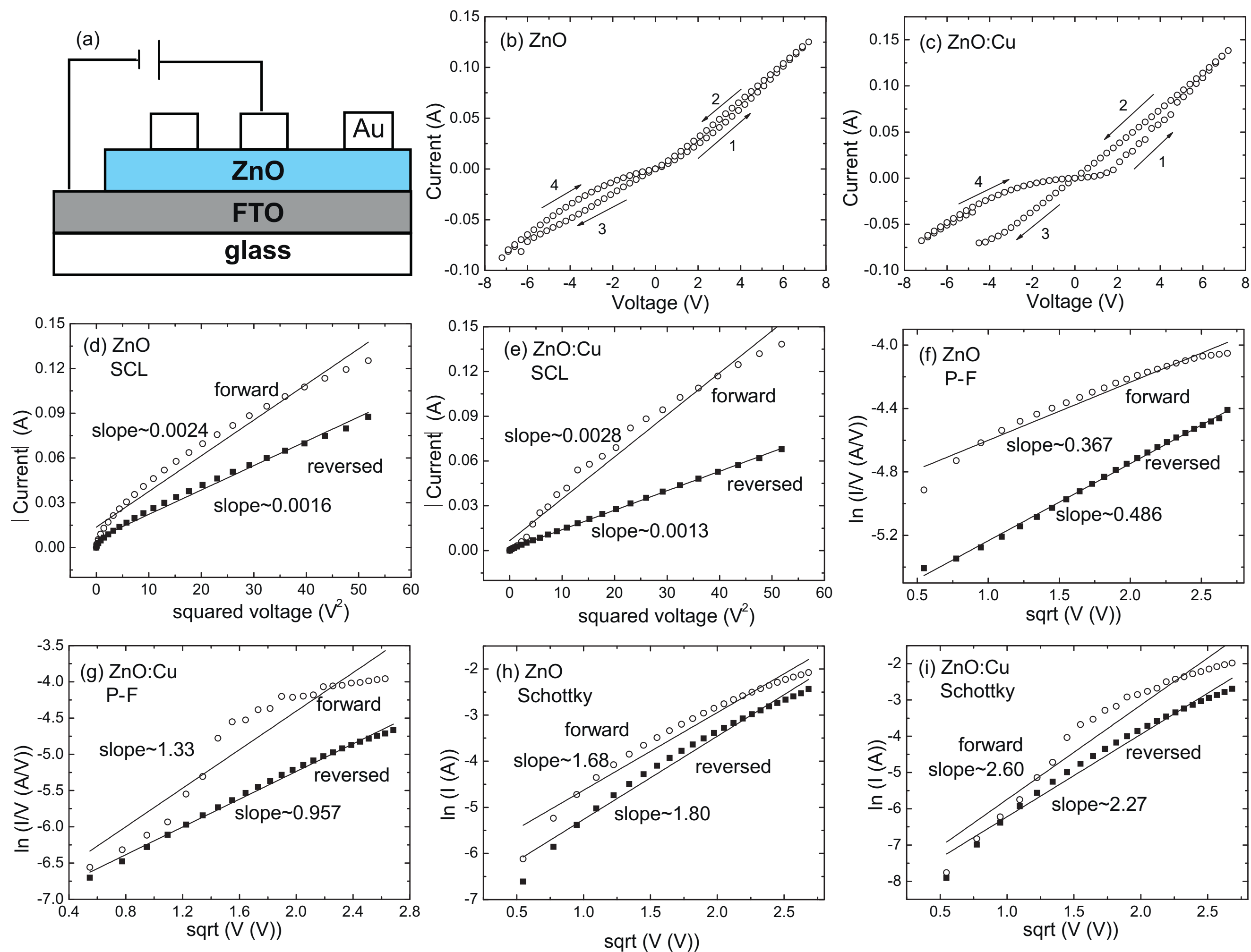


**Fig. 2.** The schematic of the test device (a); typical $I$–$V$ characteristic of RRAM cell based on Au/ZnO/FTO (b) and Au/ZnO:Cu/FTO (c) capacitors; The $I$–$V^2$ characteristics of ZnO (d) and ZnO:Cu (e) films according to SCLC mechanism at HRS; The $\ln(I/V)$–$V^{1/2}$ characteristics of ZnO (f) and ZnO:Cu (g) films according to Poole–Frenkel emission mechanism at HRS; The $\ln I$–$V^{1/2}$ characteristics of ZnO (h) and ZnO:Cu (i) films according to Schottky emission mechanism at HRS.

that of ZnO films determined by optical method [20]. So the SCL conduction mechanism can be ruled out in the present work. For P–F emission as follows, $\ln(I/V) \propto (\sqrt{e^3/\pi\varepsilon_0\varepsilon_r d}/rkT)\sqrt{V}$, where $e$ is the electronic charge, $k$ is the Boltzmann's constant, $T$ is the temperature, and $r$ is a coefficient ranging between 1 and 2, depending on the exact position of the Fermi level [18]. From the P–F emission fittings shown in Fig. 2(f and g), the relative dielectric constants for ZnO and ZnO:Cu films are derived to be 632–158 and 303–76, respectively. Thus the refractive indexes for ZnO and ZnO:Cu films are 25.1–12.6 and 17.5–8.7, respectively, with increasing $r$ from 1 to 2. They are much larger than that of ZnO films determined by optical method [20], thus the P–F emission mechanism can also be excluded. For Schottky emission, as follows: $\ln I \propto (\sqrt{e^3/4\pi\varepsilon_0\varepsilon_r d}/kT)\sqrt{\nu}$. From the Schottky emission fittings shown in Fig. 2(h and i), the relative dielectric constants for ZnO and ZnO:Cu films are derived to be 6.6 and 4.1, respectively. Thus the refractive indexes for ZnO and ZnO:Cu films are 2.5 and 2.0, respectively, which are comparable with that of ZnO films determined by optical method [20]. Therefore, the Schottky emission mechanism is valid in the present work. It should be also noted that the calculated refractive index of ZnO:Cu films is smaller than than that of ZnO films. This is in accord with the phenomenon that the ZnO:Cu films containing light ion (copper), as heavier ions usually posses larger index of refraction [21]. It has also been observed in indium doped $Bi_4Ti_3O_{12}$ films [15]. The difference in refractive index of the two materials provide a possible optical wave guide structure, in which ZnO layer can serve as a core material and ZnO:Cu layer can serve as a cladding material.

For transition metal oxides, two models of filamentary and interface conducting path are proposed to explain the resistive switching between HRS and LRS [22]. In order to separate the contributions of bulk and interface related effects, the complex impedance spectra are performed on ZnO and ZnO:Cu films under LRS and HRS states, respectively. Fig. 3(a and b) shows the typical complex impedance plane plots of ZnO and ZnO:Cu films at HRS and LRS, respectively. All these plots are almost identical in the shape of semicircle, indicating that highly conduction path does not exist according to previous report for filament based switching. If a conduction path is formed, all current flows through the path and the entirely different impedance spectra will be observed [23]. Therefore, the filament model can be excluded as switching mechanism in Au/ZnO(:Cu)/FTO structures.

It is well known that the impedance spectra in the shape of semicircle for a Schottky system can be well fitted with a simple three-element circuit composed of bulk resistance $R_b$ in series with a parallel resistor-capacitor representing the Schottky contact [24]. By fitting the experimental results of impedance spectra, the parameters of resistance and capacitance can be derived, which are summarized in Table 1. It is clear that the bulk resistance is slightly influenced by the resistance state, whereas the depletion

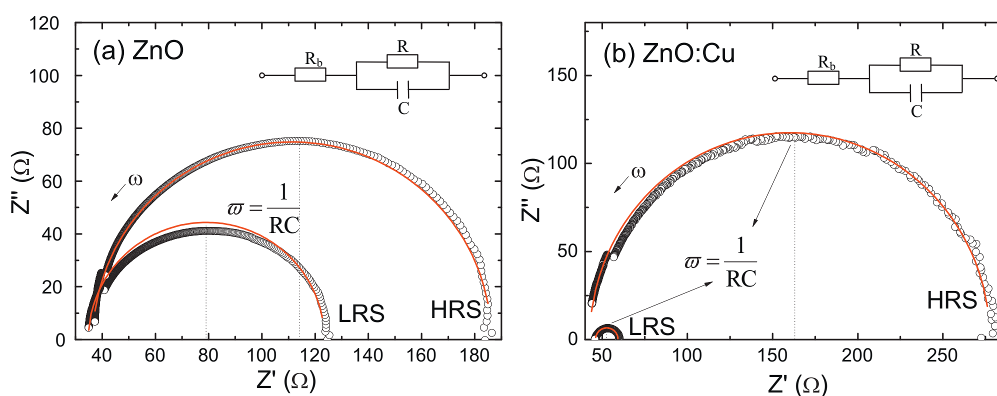


**Fig. 3.** The complex impedance spectra of Au/ZnO/FTO (a) and Au/ZnO:Cu/FTO (b) stacks under HRS and LRS. The inset shows the equivalent circuit for simulation.

**Table 1**
The fitting parameters of resistance and capacitance for ZnO and ZnO:Cu films obtained from impedance spectra recorded at HRS and LRS, respectively.

| Samples | Resistance state | $R_b$ (Ω) | $R$ (Ω) | $C$ (F) | $W_d$ (nm) |
|---|---|---|---|---|---|
| ZnO | HRS | 38 | 148 | $1.3 \times 10^{-9}$ | 1.4 |
| ZnO | LRS | 35 | 89 | $1.5 \times 10^{-9}$ | 1.2 |
| ZnO:Cu | HRS | 43 | 234 | $6.7 \times 10^{-10}$ | 1.7 |
| ZnO:Cu | LRS | 45 | 15 | $1.1 \times 10^{-8}$ | 0.1 |

layer resistance is strongly dependent on the resistance state for both ZnO and ZnO:Cu films. It means that the overall resistance in the sandwiched memory structure is dominated by the depletion layer resulting from the Schottky interface [25]. With the capacitance of a Schottky junction ($C = \varepsilon_0 \varepsilon_r S/W_d$) from impedance spectra, the depletion layer width ($W_d$) can be obtained by substituting the value of relative dielectric constant from *I–V* curve fittings [22]. The width of depletion layer are calculated to be 1.4 and 1.2 nm at HRS and LRS for ZnO, 1.7 and 0.1 nm at HRS and LRS for ZnO:Cu films, respectively, which are also listed in Table 1. The width of depletion layer at HRS is comparable to that of Ag/PCMO/Pt sandwich configuration [26]. As expected, the depletion layer at HRS is wider than that at LRS, leading to a larger resistance at HRS than that at LRS for both ZnO and ZnO:Cu films. Furthermore, the width of depletion layer of ZnO:Cu films between HRS and LRS varies much greater than that of undoped ZnO films, which is consistent with the larger ON/OFF ratio of ZnO:Cu films than that of ZnO.

In the interfacial effect, the migration of oxygen vacancies in the vicinity of the interface drives RS in various heterojunctions. Under a negative electric field, oxygen vacancies with positive charges migrate away from the Schottky-type interface between ZnO or ZnO:Cu and FTO, which widens the depletion layer, resulting in the HRS. On the other hand, with low positive voltage, the oxygen vacancies start moving toward the interface. At high positive voltage, Schottky emission of electrons into the conduction band dominates, which set the device to LRS. Therefore, the change of depletion layer width induces a reversible switching between HRS and LRS.

## 4. Conclusion

In summary, wurtzite ZnO and ZnO:Cu thin films of *c*-axis orientation have been grown on FTO substrates by pulsed laser deposition. The presence of copper in ZnO:Cu films has been confirmed by XPS. Typical bipolar reversible resistance switching effects were observed in both Au/ZnO/FTO and Au/ZnO:Cu/FTO sandwich structures, and the ON/OFF ratio increases abruptly by introducing Cu. By fitting the current-voltage curves with several conduction mechanisms, Schottky emission presents the most reasonable results, and the Cu dopant is found to reduce the refractive index of ZnO films. Based on analysis of impedance spectra at high and low resistance states of ZnO and ZnO:Cu films, the change of resistance is accompanied with the variance of the depletion width. The depletion width of ZnO films changes little, while that of ZnO:Cu films varies greatly under high and low resistance states, which is consistent with the result of that ZnO:Cu films show a much larger ON/OFF ratio than ZnO films. Therefore, the resistance switchings in ZnO and ZnO:Cu films are supposed to be due to the change of depletion width of Schottky barrier.

## Acknowledgments

This work was supported by the National Natural Science Foundation of China (Grant No. 60976016), the Program for Innovative Research Team in Science and Technology in University of Henan Province (IRTSTHN) (2012), and the Province and the Ministry Co-established Foundation of Henan University (No. SBGJ090503).

## References

[1] G.I. Meijer, Science 319 (2008) 1625.
[2] D.B. Strukov, G.S. Snider, D.R. Stewart, R.S. Williams, Nature 453 (2008) 80.
[3] Y.C. Yang, F. Pan, F. Zeng, New J. Phys. 12 (2010) 023008.
[4] U. Ozgur, Y.I. Alivov, C. Liu, A. Teke, M.A. Reshchikov, S. Dogan, V. Avrutin, S.J. Cho, H. Morkoc, J. Appl. Phys. 98 (2005) 041301.
[5] C.H. Jia, Y.H. Chen, G.H. Liu, X.L. Liu, S.Y. Yang, Z.G. Wang, J. Cryst. Growth 311 (2008) 200.
[6] T.S. Herng, D.C. Qi, T. Berlijn, J.B. Yi, K.S. Yang, Y. Dai, Y.P. Feng, I. Santoso, C. Sanchez-Hanke, X.Y. Gao, A.T.S. Wee, W. Ku, J. Ding, A. Rusydi, Phys. Rev. Lett. 105 (2010) 207201.
[7] J.B. Kim, D. Byun, S.Y. Ie, D.H. Park, W.K. Choi, J.W. Choi, B. Angadi, Semicond. Sci. Technol. 23 (2008) 095004.
[8] X.B. Wang, D.M. Li, F. Zeng, F. Pan, J. Phys. D: Appl. Phys. 38 (2005) 4104.
[9] T. Ghosh, D. Basak, J. Phys. D: Appl. Phys. 42 (2009) 145304.
[10] T. Ghosh, M. Dutta, S. Mridha, D. Basak, J. Electrochem. Soc. 156 (2009) H285.
[11] A. Furukawa, N. Ogasawara, R. Yokozawa, T. Tokunaga, Jpn. J. Appl. Phys. 47 (2008) 8799.
[12] A. Hartmann, M.K. Puchert, R.N. Lamb, Surf. Interface Anal. 24 (1996) 671.
[13] H.L. Pan, B. Yao, T. Yang, Y. Xu, B.Y. Zhang, W.W. Liu, D.Z. Shen, Appl. Phys. Lett. 97 (2010) 142101.
[14] H.W.P. Carvalho, A.P.L. Batista, P. Hammer, T.C. Ramalho, J. Hazard. Mater. 184 (2010) 273.
[15] C.H. Jia, Y.H. Chen, L.H. Ding, W.F. Zhang, Appl. Surf. Sci. 253 (2007) 9506.
[16] R. Waser, R. Dittmann, G. Staikov, K. Szot, Adv. Mater. 21 (2009) 2632.
[17] H.Y. Peng, G.P. Li, J.Y. Ye, Z.P. Wei, Z. Zhang, D.D. Wang, G.Z. Xing, T. Wu, Appl. Phys. Lett. 96 (2010) 192113.
[18] J.R. Yeargan, H.L. Taylor, J. Appl. Phys. 39 (1968) 5600.
[19] H. Yang, H. Wang, G.F. Zou, M. Jain, N.A. Suvorova, D.M. Feldmann, P.C. Dowden, R.F. Depaula, J.L. MacManus-Driscol, A.J. Taylor, Q.X. Jia, Appl. Phys. Lett. 93 (2008) 142904.
[20] M.A.M. Khan, M.W. Khan, M. Alhoshan, M.S. Alsalhi, A.S. Aldwayyan, Appl. Phys. A. 100 (2010) 45.

[21] Y.M. Tsau, Y.C. Chen, H.F. Cheng, I.N. Lin, J. Eur. Ceram Soc. 21 (2001) 1561.
[22] A. Sawa, Mater. Today 11 (2008) 28.
[23] Y.H. You, B.S. So, J.H. Hwang, W. Cho, S.S. Lee, T.M. Chung, C.G. Kim, K.S. An, Appl. Phys. Lett. 89 (2006) 222105.
[24] D.A. Scrymgeour, C. Highstrete, Y.J. Lee, J.W.P. Hsu, M. Lee, J. Appl. Phys. 107 (2010) 064312.
[25] J. Lee, E.M. Bourim, D. Shin, J.S. Lee, D.J. Seong, J. Park, W. Lee, M. Chang, S. Jung, J. Shin, H. Hwang, Curr. Appl. Phys. 10 (2010) e68.
[26] S. Tsui, A. Baidalov, J. Cmaidalka, Y.Y. Sun, Y.Q. Wang, Y.Y. Xue, C.W. Chu, L. Chen, A.J. Jacobson, Appl. Phys. Lett. 85 (2004) 317.